Volume 36

http://acousticalsociety.org/

177th Meeting of the Acoustical Society of America

Louisville, Kentucky 13-17 May 2019

Physical Acoustics: Paper 4pPAb9

A prototype soundproof box for isolating ground-air seismo-acoustic signals

Eric J. Lysenko and Tracianne B. Neilsen
Department of Physics and Astronomy, Brigham Young University, Provo, Utah, 84602; eric.lysenko@yahoo.com; tbnbyu@gmail.com

Robin S. Matoza

Department of Earth Science, University of California, Santa Barbara, Santa Barbara, CA, 93106; rmatoza@ucsb.edu

Wave conversion and transmission at the interface between solid earth and fluid atmosphere result in airground and ground-air seismic and acoustic (seismo-acoustic) coupling. Seismo-acoustics is particularly relevant in observational geophysics; networks of seismic instrumentation are increasingly collocated with infrasonic pressure sensors and used in the study of a wide array of natural and anthropogenic sources. Two field experiments were carried out to isolate the ground-air converted signal from subaerial explosions. One experiment used 17" balloons filled with a stoichiometric oxy-acetylene mix placed on the ground, and another used Pentex configured at depths of 30 and 60 cm. Ground-radiated signals were isolated with a portable soundproof box constructed of mass-loaded vinyl, soundproofing composite board, liquid nails and wood glue to dampen air-borne sound waves. Random incidence insertion loss of the box was estimated and applied to signals measured outside the box. These filtered signals are compared with the signals observed from a microphone placed inside the box. Preliminary analysis shows evidence of ground radiated signals detected in the Pentex experiment, but not in the balloon experiment. These observations need confirmation with additional seismic and infrasonic signal processing methods. However, preliminary results suggest a viable technique for isolating ground-borne acoustic waves.



1. INTRODUCTION

Volcanic eruptions pose a serious threat to operating aircraft, since ejecta from volcanoes have a lower melting point than the operating temperature of aircraft engines (Matoza *et al.* 2018a). For example, during the 2010 eruption of the Icelandic volcano Eyjafjallajökull, the ash cloud climbed almost 9 km into the atmosphere causing most of the European airspace to close for six days. The proximity of this relatively small volcanic eruption to numerous major airports caused the largest disruption of air travel since World War II. Currently, satellites are used for visual confirmation of volcanic eruptions and estimation of how much ejecta and vapor is released into the atmosphere.

Recent research has focused on using infrasound from volcanoes for early volcanic eruption detection. The ability to interpret volcano infrasound has the potential to not only reduce the time to confirm an eruption but also indicate the type and amount of ejecta (Matoza *et al.* 2018a). Infrasound can travel thousands of kilometers due to low atmospheric absorption and atmospheric refraction effects.

Previous research has shown connections between infrasound and volcanic eruptions. Studies have characterized the sound from Strombolian (Vergniolle and Brandeis 1994 and 1996, Jolly *et al.* 2017), Plinian (Fee *et al.* 2010a), and Vulcanian explosions (Matoza *et al.* 2018b, Anderson *et al.* 2018, Marchetti 2009), as well as degassing explosions (Johnson and Lees 2000), volcanic tremors (Fee *et al.* 2010b, Fee *et al.* 2017a), and rock fall (Moran *et al.* 2008). Connections have also been made between infrasound and eruption mass (Fee *et al.* 2017b), velocity (McKee *et al.* 2017) and plume height (Caplan-Auerbach *et al.* 2010). The infrasound from volcanic jetting—multiphase and turbulent fluid jets erupting explosively from a vent—has been shown to have the same statistical distribution as the noise from solid rocket motors and afterburning military aircraft (Matoza *et al.* 2013).

Apart from taking direct measurements of volcanic infrasound, researchers can use scale-model eruptions to approximate the acoustic and seismic signals generated by different types of volcanic blasts. These experiments have in some cases used explosives that are buried, sometimes underneath ground that has been shaped into a crater. Scale model explosions provide a controlled, predictable way to investigate volcanic eruptions. Examples of scale-model experiments have been reported in Bowman *et al.* (2014), Ohba *et al.* (2002), Spina *et al.* (2018), and Taddeucci *et al.* (2014).

In Summer 2018, we participated in two scale-model explosion experiments: one with oxyacetylene-filled balloons and another with buried Pentex explosives. The purpose of these experiments was to record the acoustic signal from explosives in various configurations and ascertain the effect of crater size and scaled depth of burial on the acoustic signal. The data and analysis of these scale-model experiments will hopefully help characterize volcanic eruptions from the infrasound they emit.

This paper focuses on one of our goals from the scale-model experiments: taking direct measurements of seismo-acoustic coupling. Coupling, in this context, refers to the transference of vibrational energy from one medium into another. We were interested in how the vibrations traveling in the ground couple into airborne sound. A microphone was placed in a sound-proof box, constructed to dampen airborne vibrations. While no "extra" noise was detected in the box from the balloon explosions that would indicate coupling, the microphone in the buried Pentex test picked up more energy than could have reached it via airborne propagation paths, which is indicative of ground-air coupling.

2. SEISMO-ACOUSTIC COUPLING

Seismo-acoustic coupling is the transfer of acoustic energy between ground-borne and airborne vibrations, or vice versa (Arrowsmith et al. 2010). Significant research has been done to investigate acoustically induced seismic waves as in the work of Sabatier et al. (1986) and Hickey and Sabatier (1997). Evidence of both types of seismo-acoustic coupling can be found by examining the cross-correlation (Ichihara *et al.* 2012) and coherence (Matoza *et al.* 2018b) between the vertical seismic velocity and infrasound signals, as well as the alignment of the vertical seismic displacement with the infrasound (Matoza *et al.* 2019).

Both types of coupling have been studied on regional and local scales (Matoza *et al.* 2018b). Air-ground coupling measurements are used to monitor eruption tremors (Matoza and Fee 2014) and eruption detection at the Alaska Volcano Observatory (Fee *et al.* 2016). The frequency dependence of air-ground coupling has also been studied (Bass *et al.* 1980). Ground-air coupling from compressional and shear seismic waves and leaky Rayleigh waves have also been identified (Matoza *et al.* 2009) and are an important link in relating infrasonic signatures with specific types of volcanic eruptions (Matoza *et al.* 2014). Ground-air coupling from these sources has also been used for signal detection and localization (Mckee *et al.* 2018). An example of how ground-air coupling is modeled is provided in Figure 10 of Matoza *et al.* (2009). It shows the outward propagation of a seismic wave and the airborne acoustic waves that result from coupling. Evidence from ground-air coupling also comes from meteoroid impact (Edwards et al. 2007) and earthquakes (Donn and Posmemtier, 1964, Mutschlecner and Whitaker 2005).

In the remainder of this paper we focus on ground-air seismo-acoustic coupling and a possible means of measuring it. Detecting and quantifying ground-air coupling is a necessary component of early volcanic detection (Matoza, 2018b). Our experiments explore coupling to see if it is a measurable source of acoustic energy in the scale-model experiments by using a portable soundproof box that significantly reduces airborne sound.

3. EXPERIMENTAL METHODS

Plans for measuring seismo-acoustic coupling are reported in this section. First, information regarding the plan, design, and construction of our soundproof box is presented. Next we explain why and how we measured the insertion loss of the box. Lastly, both field tests are described.

A. SOUNDPROOF BOX

We constructed a portable soundproof box to insulate a microphone from airborne waves and thus, isolate ground-air coupled waves. Figure 1 illustrates how airborne waves from an explosion encountering the surface of the apparatus are reflected and deadened, thereby allowing the microphone housed within the box to detect ground-air coupled waves.

The box was constructed of various soundproofing materials to incorporate high mass, mechanical decoupling, and absorption. The box was composed of 20-lb of mass loaded vinyl (MLV) with a density of 1-lb/ft², 4-ft² of soundproofing board, liquid nails and wood glue to glue the soundproofing boards together, and duct tape to keep the MLV from sliding out of the box (exact instructions for making the box are found in Lysenko 2019). The large quantity of MLV is responsible for the high mass, which is necessary for noise deadening. A mechanical decoupling effect was created by placing the MLV sheets tightly between an inner and outer shell of soundproofing board without adhesive. Absorption was included by using soundproofing boards for the inner and outer shells of the box. The box was approximately 1' x 1' x 8". The MLV penetrated past the base of the soundproofing board by 2". Approximately 2" of MLV sits between 3/4" soundproofing boards that constitute each shell. Figure 2 shows bottom and side views of the box.

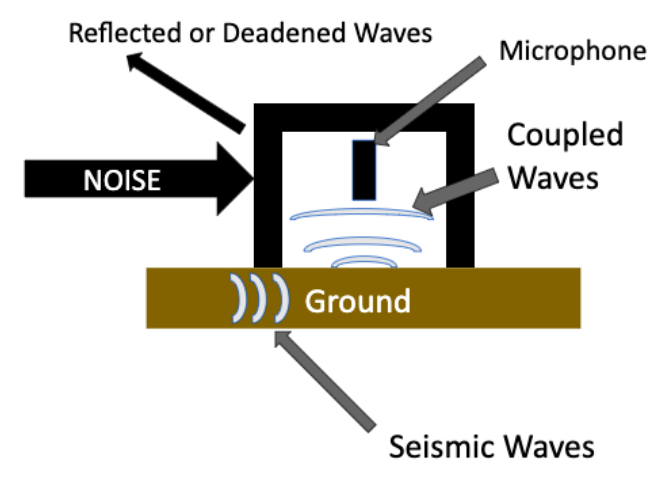


Figure 1 – Illustration showing attenuation of airborne acoustic waves and presence of ground-air acoustic coupling within the box.

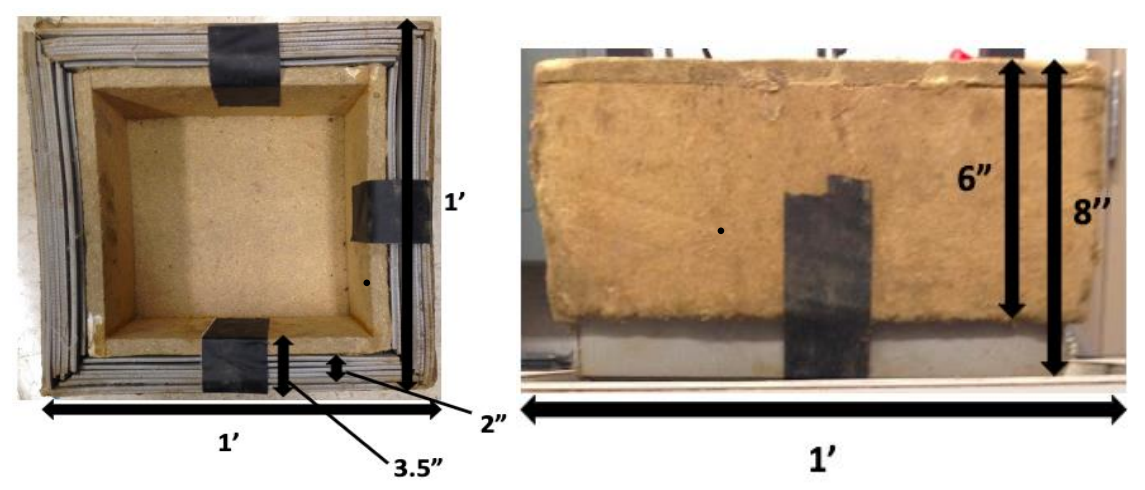


Figure 2- Bottom and side views of the box. Duct tape was used to keep the MLV sheets from sliding out.

B. INSERTION LOSS

The random insertion loss of this box was estimated to determine its ability to deaden airborne sounds. The random insertion loss represents the frequency-dependent filtering effect the box has on airborne noise and estimates the difference between signals received by microphones inside and outside of the box.

The random insertion loss was estimated in BYU's reverberation chamber. We used a starter pistol as the impulsive signal, a microphone inside the box, and three adjacent microphones. The edges of the box were insulated with a memory foam pad, and a concrete block was added on top of the box to fully compress the foam, as shown in Figure 3. The test was carried out with and without a concrete weight on top of the box to approximate upper and lower bounds of noise filtering based on the seal around the base of the box. All microphones were ½" GRAS, prepolarized, free-field microphones that were suspended with the diaphragm approximately 1/8" above the ground using small inverted tripods.

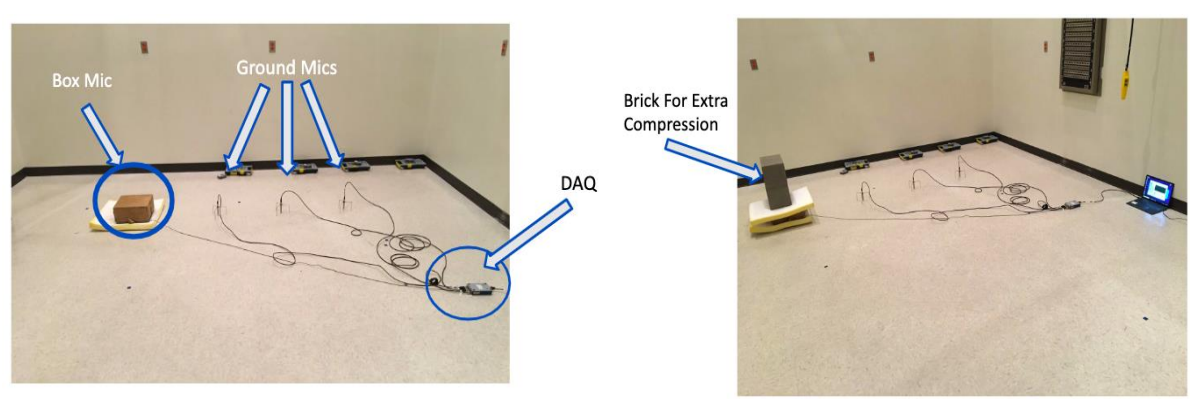


Figure 3- Setup in the reverberation chamber: (left) without and (right) with a concrete block on top of the box.

Multiple types of software were employed to collect and analyze the data. Measurements were recorded with a National Instruments 9234 with a 51.2 kHz sampling rate and LabView Software developed by Kent Gee and collaborators, called Acoustic Field Recorder. The recordings of the starter pistol shots were used to obtain one-third octave (OTO) band spectra with MATLAB. The OTO band spectra for the different microphones are shown in Figure 4: The case with the concrete block is shown on the left, and the one without the concrete block on the right.

The OTO band spectra plots in Figure 4 show how effectively the box filters noise with and without a concrete weight to help insulate the base. With the concrete on the box (left graph), the box begins filtering noise around 20 Hz and improves its sound filtering linearly as frequency increases. Without the concrete on the box (right graph), the box appears to begin filtering noise at approximately 60 Hz and provides less reduction in overall sound level. These data are used to estimate the insertion loss of the system.

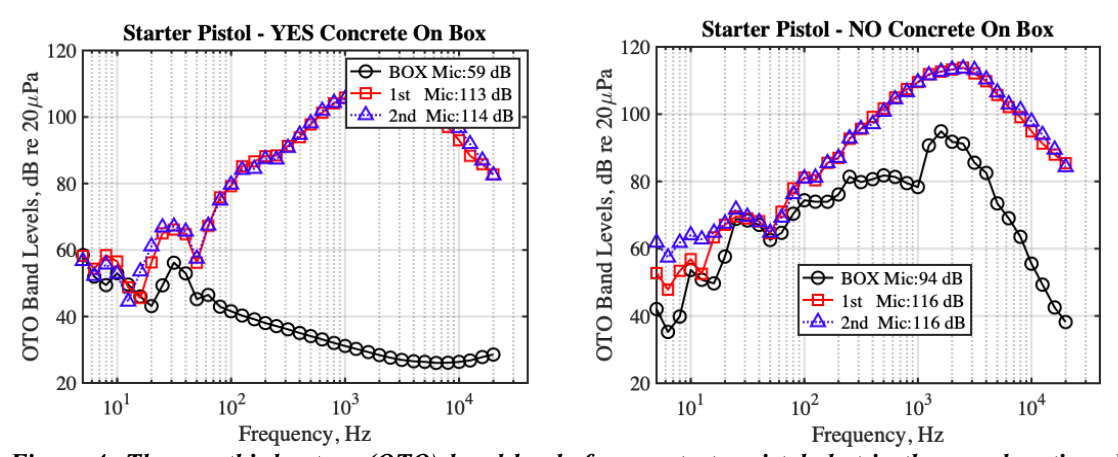


Figure 4- The one-third-octave (OTO) band levels from a starter pistol shot in the reverberation chamber. The black lines show the OTO band levels of the microphone in the box.

The random incidence insertion loss is estimated from the measured narrow band spectra. The insertion loss is calculated as

$$IL(f) = 10 * \log_{10} \left[\frac{P_T(f)}{P_R(f)} \right],$$

where P_T is the spectrum without an enclosure and P_R is the spectrum with an enclosure. The signal from the box is given as P_R , and the average signal from the three outer microphones is given as P_T . (The similarity in the spectra of the outer microphones in Figure 4 implies that the sound field near the floor is diffuse in the reverberation chamber, so this method is similar to taking a measurement at a single location with and without the box.) By calculating IL for the data with and without the concrete block on the box, we can estimate the upper and lower bounds of insertion loss as shown in Figure 5. Because of the jagged nature of the insertion loss in the narrowband spectra (black), we used MATLAB's 'smooth' function to generate a smoother narrowband curve (cyan) to apply to signals in our tests. The lower bound of insertion loss (right plot)—when subtracted from the signal outside of the box—gives a generous upper threshold to determine if there is extraneous sound in the box (see Figure 10). This extra sound can be interpreted as evidence of ground-air coupling in our experiments.

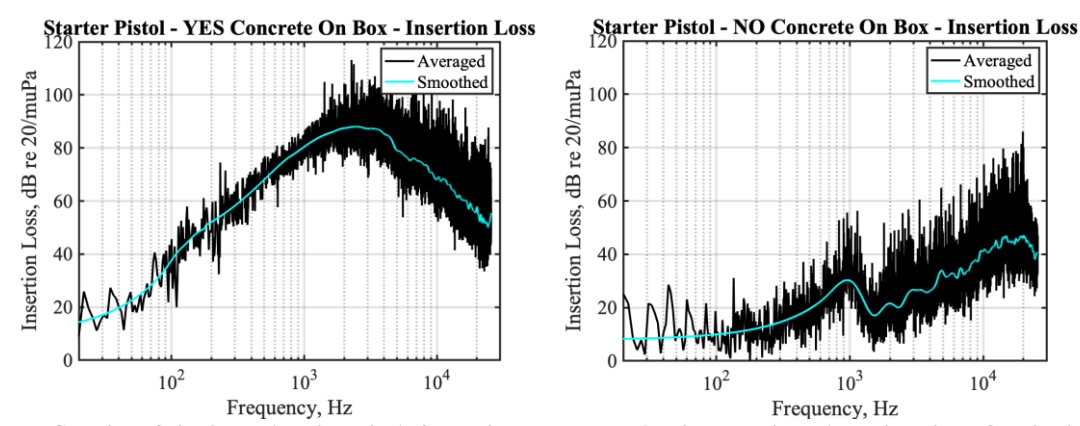


Figure 5- Graphs of the insertion loss (IL) from the two setups in the reverberation chamber. On the left, the IL with concrete weight on the box provides an upper bound on insertion loss. On the right, the IL without concrete provides a generous lower bound on the IL.

C. EXPLODING BALLOON TEST

Our first field test used balloons filled with a stoichiometric oxy-acetylene mix to create large explosions. These exploding balloons generate large shock waves, as reported by Young et al. (2015) and Leete et al. (2015), making them ideal for our test. The balloons were detonated via radio transmitter connected to a model rocket ignition match. The balloons were placed on the ground, as shown in Figure 6. The plastic wrap was used to keep them from popping on the grass or from being blown away. The soundproof box was placed 100 m away from the blast along a linear array, and an additional ground microphone was placed 1 m to the side of the box to compare the signals inside and outside of the box.



Figure 6 – Balloon shown on ground covered in plastic wrap to keep it from popping on the grass and also to prevent it from moving.

The box microphone and the adjacent ground microphone were $\frac{1}{2}$ " GRAS pre-polarized free-field microphones. These microphones had a frequency response (\pm 2 dB) from 3.15 Hz to 20 kHz, a dynamic range of 15 dB(A) to 148 dB, and \sim 56 mV/Pa sensitivity. Each was set in an inverted tripod as shown in Figure 7-left. The microphone in the box sat inside a 6 in deep square hole that the box could fit in, as shown in Figure 7-center. The hole was then covered by the box and dirt was packed tightly around the sides (Figure 7-right). The acoustic signals were recorded with a National Instruments PXI-1042 data acquisition system at 204.8 kHz sampling rate.



Figure 7- (Left) A ground microphone in an inverted tripod that was placed next to the box. (Center) A ground mic in an inverted microphone in the uncovered box hole. (Right) The box partially buried in the ground.

D. VOLCANO HAZARDS WORKSHOP

Our second experiment was an NSF-funded Volcano Hazards Workshop hosted by the University of Buffalo at their Geohazards Field Station. Researchers from several universities joined together to make a variety of measurements. The buried charges were made of 90 grams Pentex (mix of PETN and TNT). Each had an energy of 0.437 MJ. They were buried at depths of approximately 30 and 60 cm. Each test included six detonations in sequence (0.5 sec apart). The burial configuration and order of detonation varied between the tests to replicate various volcanic craters and eruption types. A photograph of a detonation is shown in Figure 8 (middle).

Data for the Volcano Hazards Workshop was collected with the same microphones as the Exploding Balloon Test, and in a similar configuration. The box was placed 30 m away from the center of the test site and buried (Figure 8- left). An inverted microphone was placed near the ground adjacent to the box to calculate insertion loss for the first two tests, and elevated microphones at 0.35 m and 3 m were 1 m from the box, and one meter off the ground, as illustrated in Figure 8 (right).



Figure 8- (Left) Buried soundproof box housing a microphone to detect seismic-acoustic coupling. (Middle) One of the six explosions from the second test (Pad 2)- Photo courtesy of Jacopo Taddeucci. (Right) A schematic of the sensor configuration.

4. RESULTS AND ANALYSIS

The data from the Exploding Balloon Test and Volcano Hazards Workshop are shown and potential indications of seismo-acoustic coupling analyzed. The signals are transformed into sound pressure level (SPL). The estimated random incidence insertion loss of the soundproof box is then applied to the ground microphone signal (outside the box) in each test. These modified signals are compared to the signals received inside the soundproof box to determine if coupling took place. Results are shown as narrowband and OTO band spectra for clarity.

A. EXPLODING BALLOON TEST

Our first step was to analyze the pressure waveform plots from the test to see how the signal received on the microphone in the box compared to that outside the box. Figure 9 shows the pressure waveform received in the ground microphones outside (red) and inside (black) the box when a 17" balloon was detonated. The plot shows that the box dampened a significant amount of the air-born sound. However, the waveforms alone do not tell us if the sound in the box is due to the filtering effect of the box or if ground-air coupling in present. To answer this question, the spectra of the sound inside and outside the box must be compared by considering the insertion loss of the box.

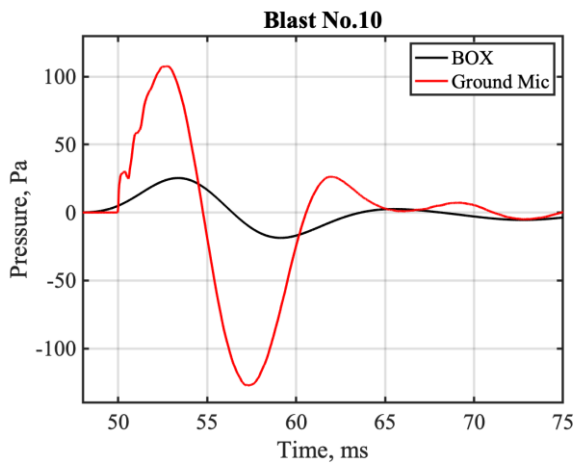


Figure 9- Waveforms of a 17 in exploding balloon blast measured on a microphone inside the box (black) and outside the box (red) at a distance of 100m.

The estimated upper and lower bounds of insertion loss (for the with and without concrete cases) are applied to the spectra measured outside the box. If the box signal lies between these upper and lower bounds, the signal inside the box can be considered a filtered version of the airborne noise. Conversely, if the box signal is above the bounds on filtered signals, the extra sound in the box is likely due to ground-air coupling. Figure 10 shows the SPL (Sound Pressure Level) and OTO (one-third-octave) band levels of the ground mic signal with the insertion loss applied. The OTO box signal in Figure 10 (shown as black squares) lies between the filtered spectrum from the lower and upper bounds of insertion loss, which are shown with the blue triangles and green inverted triangles, respectively. (The bounded spectra begin at 20 Hz because IL approaches zero

rapidly below 20 Hz.) The box appears to receive another source of sound for frequency > 8 kHz; the excess high-frequency energy in the box could be due to scattering.

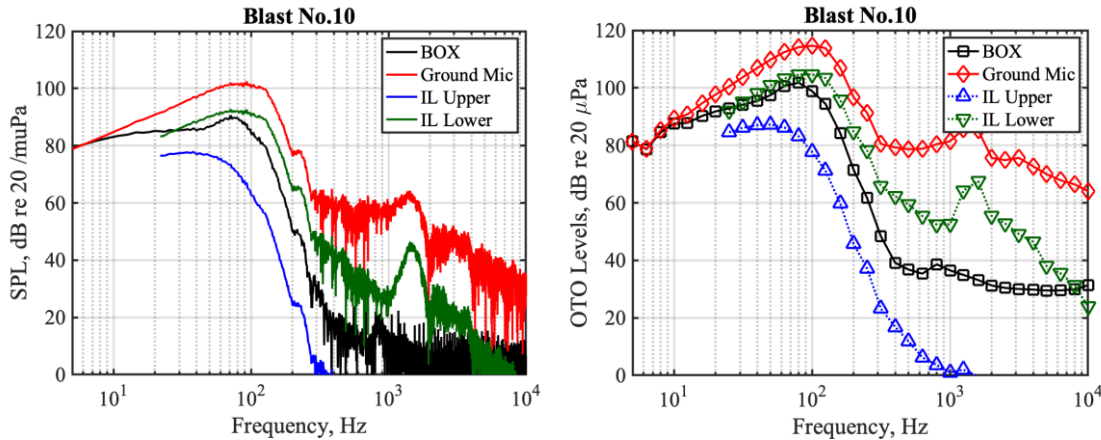


Figure 10 – Comparison of SPL (left) and OTO band levels (right) from a 17 in exploding balloon measured in the box (black) with those measured outside the box (red) and filtered spectra using the upper and lower bounds on the estimated insertion loss. The OTO band is included for clarity.

B. VOLCANO HAZARDS WORKSHOP

At the Volcano Hazards Workshop, our goal was to compare the pressure waveforms and spectra inside and outside the box for evidence of ground-air coupling. Pressure waveforms for the Volcano Hazards Workshop are shown in Figure 11. The pressure received on the ground mic (red) and the pressure on the box mic (black) are significantly different. As in the Exploding Balloon Test, we applied the insertion loss to the corresponding spectra measured outside the box to estimate the filtering effect of the box.

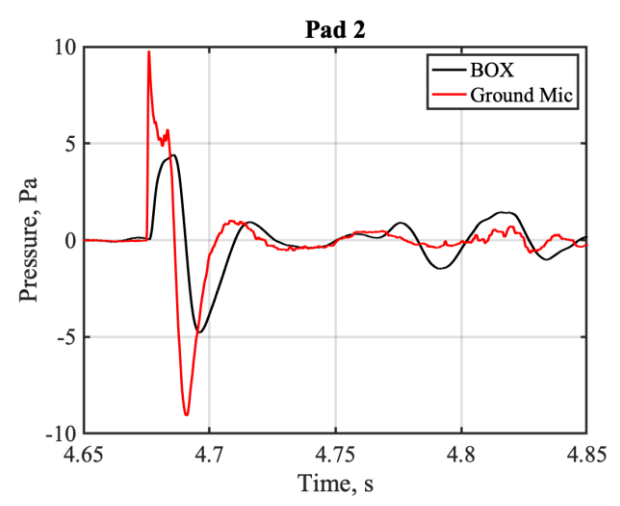


Figure 11 – Waveforms from Volcano Hazards Test (second blast on Pad 2) measured on microphones inverted above the ground outside (black) and inside (red) the box at a distance of approximately 30 m.

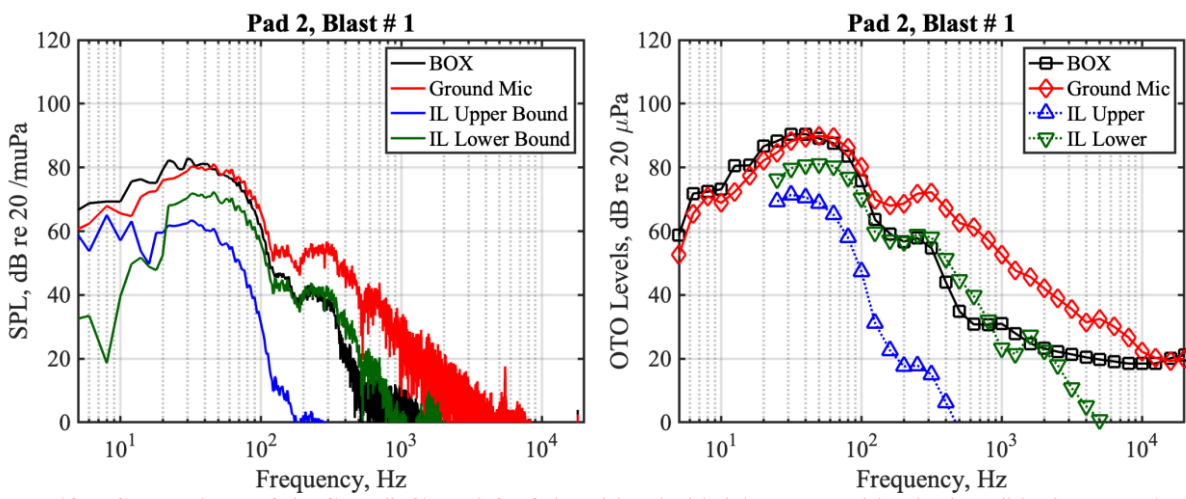


Figure 12 – Comparison of the SPL (left) and OTO band levels (right) measured in the box (black squares) with those measured outside the box (red diamonds) and filtered spectra from the upper and lower bounds on the estimated insertion loss bounds.

The estimated insertion loss bounds are applied to the spectrum from the microphone outside the box and compared to the spectrum inside the box to look for evidence of ground-air coupling. The measured and filtered SPL and OTO band levels of our signals are shown in Figure 12, as well as upper and lower bounds of the filtered spectra due to insertion loss. In both graphs, the spectral content in the box exceeds that expected (due to filtering) below 100 Hz, which we claim is evidence of ground-air coupling for this buried explosive blast. In the 100-300 Hz band, the spectrum in the box is basically the same as the upper bound on the filtered spectra, making it hard to identify the upper frequency limit for the coupling.

C. UNCERTAINTY

While preliminary evidence of ground-air coupling is shown in Figure 12, sources of uncertainty need to be taken into account. First, vibrations of the tripod could be transmitted into the microphone to generate extraneous noise, particularly because of the orientation of the microphone. However, the microphone outside of the box would have experienced the same vibrations, making this a systematic error. Since our results are based on comparison of the two signals, the effects of the tripod vibrations are likely mediated. Second, the box has resonances between 800-1500 Hz, as seen on the left plot of Figure 5. Because these frequencies are much higher than those at which we are trying to detect the coupling, we do not think box resonances have a significant bearing on our results. Third, the smoothing function used for our narrowband IL could have been replaced by different band processing to include larger frequency bins to be more accurate. Fourth, reflections from the box were possibly received on the ground microphone, and scattering effects from the tripod legs could have played a role—especially at higher frequencies. Lastly, our box was in contact with the ground and likely received vibrations from the passing seismic waves. The box vibrations could have coupled with the air to produce sound picked up by our box microphone. Additional tests would be needed to distinguish boxradiated noise from ground-radiated noise.

5. CONCLUSION

The goal of this work was to construct and use a sound-proof box to identify ground-air seismo-acoustic coupling from scale-model volcanic explosions. The box was constructed as a portable means to measure coupling in the field by comparing microphone signals within and

without the box. We applied this method to two field tests: one with exploding oxy-acetylene balloons and another with buried explosives. The blasts were detonated in various configurations, and the waveforms and spectra were compared. Random incidence insertion loss for the box was estimated to bound its filtering effects. The insertion loss was then applied to the spectrum measured outside the box to give an estimate of bounds for the filtered spectra due to airborne noise.

The two field tests gave different results. The spectrum inside the box from the explosion of a 17" oxy-acetylene balloon falls within the upper and lower bounds of the filtered spectrum expected from the box's estimated insertion loss. From this it appears that seismic waves from the explosion of the 17" balloon lying on the ground did not couple with the air. A comparison with the additional data taken during these experiments for balloons placed in craters as well as larger balloons might show a different effect.

The spectrum inside the box during one of the louder blasts at the Volcano Hazards Workshop lies above the upper bounds of filtered spectrum. Thus, the box appears to have detected ground-air coupled waves in the Volcano Hazards Workshop. Although there are sources of experimental uncertainty, this detection appears to agree with preliminary cross correlation and coherence analyses of the seismic and acoustic signals (Neilsen *et al.* 2019). The multiple tests with different blast configurations need to be analyzed to see if a relationship between the seismic amplitude and the seismo-acoustic coupling can be found.

ACKNOWLEDGEMENTS

We would like to thank the Brigham Young University Office of Research and Creative Activities and the Mentoring Environment Grant for funding our experiments and the College of Physical and Mathematical Sciences for an undergraduate research assistantship. We would like to thank Robin Matoza and his research group for encouraging us to take these measurements. The experiments for the Volcano Hazards Workshop were conducted at the University at Buffalo's Geohazards Field Station as part of a workshop on large-scale experiments in volcanology. Financial support for the workshop was from NSF (Grant EAR 1420455) and the UB Center for Geohazards Studies. We appreciate Greg Valentine, Ingo Sonder, and Andrew Harp at the University of Buffalo for their support in this endeavor. We are grateful to Kent Gee for the loan of his equipment and to Jeremy Peterson for making the inverted tripods. Lastly, we would like the thank the additional BYU undergraduate students that helped with the experiments: Carla Butts, Julio Escobedo, Menley Hawkes, Christian Lopez, Margaret McKay, and Sarah Shaw.

REFERENCES

Anderson, J. F., Johnson, J. B., Steele, A. L., Ruiz, M. C., & Brand, B. D. (2018). "Diverse eruptive activity revealed by acoustic and electromagnetic observations of the 14 July 2013 intense vulcanian eruption of Tungurahua Volcano, Ecuador". *Geophys. Res. Lett.*, 45, 2976–2985.

Arrowsmith, S.J., Johnson, J.B., Drob, D.P. and Hedlin, M.A., (2010). "The seismoacoustic wavefield: A new paradigm in studying geophysical phenomena". Rev. Geophys., 48(4).

Bass, H. E., Bolen, L. N., Cress, D., Lundien, J., & Flohr, M. (1980). "Coupling of airborne sound into the earth: frequency dependence". J. Acoust. Soc. Am., 67(5), 1502-1506.

Bowman, D. C., Taddeucci, J., Kim, K., Anderson, J. F., Lees, J. M., Graettinger, A. H., ... & Valentine, G. A. (2014). "The acoustic signatures of ground acceleration, gas expansion, and spall fallback in experimental volcanic explosions". *Geophys. Res. Lett.*, 41(6), 1916-1922.

Caplan-Auerbach, J., Bellesiles, A., & Fernandes, J. K. (2010). "Estimates of eruption velocity and plume height from infrasonic recordings of the 2006 eruption of Augustine Volcano, Alaska". J. Volcanol. Geotherm. Res., 189(1-2), 12-18.

Donn, William L., and Eric S. Posmentier (1964). "Ground-coupled air waves from the great Alaskan earthquake." *J. Geophys. Res.* 69(24) 5357-5361.

Edwards, W. N., Eaton, D. W., McCausland, P. J., ReVelle, D. O., & Brown, P. G. (2007). "Calibrating infrasonic to seismic coupling using the Stardust sample return capsule shockwave: Implications for seismic observations of meteors". *J. Geophys. Res.*: Solid Earth, 112(B10).

Fee, D., Garces, M., & Steffke, A. (2010a). "Infrasound from Tungurahua Volcano 2006–2008: strombolian to plinian eruptive activity". *J. Volcanol. Geotherm. Res.*, 193(1-2), 67-81.

Fee, D., Steffke, A., & Garces, M. (2010b). "Characterization of the 2008 Kasatochi and Okmok eruptions using remote infrasound arrays". *J. Geophys. Res. Atmos.*, 115(D2).

Fee, D., Haney, M., Matoza, R., Szuberla, C., Lyons, J., & Waythomas, C. (2016). "Seismic envelope-based detection and location of ground-coupled airwaves from volcanoes in Alaska". *Bull. Seismol. Soc. Am.*, 106(3), 1024-1035.

Fee, D., Haney, M. M., Matoza, R. S., Van Eaton, A. R., Cervelli, P., Schneider, D. J., & Iezzi, A. M. (2017a). "Volcanic tremor and plume height hysteresis from Pavlof Volcano, Alaska". *Science*, 355(6320), 45-48.

Fee, D., Izbekov, P., Kim, K., Yokoo, A., Lopez, T., Prata, F., ... & Iguchi, M. (2017b). "Eruption mass estimation using infrasound waveform inversion and ash and gas measurements: evaluation at Sakurajima Volcano, Japan". *EPSL*, 480, 42-52.

Hickey, Craig J., and James M. Sabatier (1997). "Measurements of two types of dilatational waves in an air-filled unconsolidated sand." *J. Acoust. Soc. Am.*, 102(1), 128-136.

Ichihara, M., Takeo, M., Yokoo, A., Oikawa, J., and Ohminato, T. (2012). "Monitoring volcanic activity using correlation patterns between infrasound and ground motion". *Geophys. Res. Lett.*, 39, L04304.

Johnson, J. B., & Lees, J. M. (2000). "Plugs and chugs—seismic and acoustic observations of degassing explosions at Karymsky, Russia and Sangay, Ecuador". *J. Volcanol. Geotherm. Res.*, 101(1-2), 67-82.

Jolly, A. D., Matoza, R. S., Fee, D., Kennedy, B. M., Iezzi, A. M., Fitzgerald, R. H., ... & Johnson, R. (2017). "Capturing the acoustic radiation pattern of strombolian eruptions using infrasound sensors aboard a tethered aerostat, Yasur Volcano, Vanuatu". *Geophys. Res. Lett.*, 44(19), 9672-9680.

Leete, K. M., Gee, K. L., Neilsen, T. B., & Truscott, T. T. (2015). "Mach stem formation in outdoor measurements of acoustic shocks". J. Acoust. Soc. Am., 138(6), EL522-EL527.

Lysenko, Eric (2019)." Direct measurement of seismo-acoustic wave coupling". Senior Thesis, Department of Physics and Astronomy, Brigham Young University, Provo, UT

Marchetti, E., Ripepe, M., Harris, A. J. L., & Delle Donne, D. (2009). "Tracing the differences between vulcanian and strombolian explosions using infrasonic and thermal radiation energy". *EPSL*, 279(3-4), 273-281.

Matoza, R. S., Garcés, M. A., Chouet, B. A., D'Auria, L., Hedlin, M. A., Groot-Hedlin, D., & Waite, G. P. (2009). "The source of infrasound associated with long-period events at Mount St. Helens". *J. Geophys. Res.*, 114(B4).

Matoza, R. S., Fee, D., Neilsen, T. B., Gee, K. L., & Ogden, D. E. (2013). "Aeroacoustics of volcanic jets: acoustic power estimation and jet velocity dependence". *J. Geophys. Res.*, 118(12), 6269-6284.

Matoza, R. S., and Fee, D. (2014). "Infrasonic component of volcano-seismic eruption tremor". Geophys. Res. Lett., 41, 1964–1970.

Matoza, R. S, & Fee, D. (2018a). "The inaudible rumble of volcanic eruptions". Acoustics Today, 14(1).

Matoza, R. S., Fee, D., Green, D. N., Le Pichon, A., Vergoz, J., Haney, M. M., ... & McKee, K. (2018b). "Local, regional, and remote seismo-acoustic observations of the April 2015 VEI 4 eruption of Calbuco volcano, Chile". *J. Geophys. Res.*, 123(5), 3814-3827.

Matoza, R. S., Arciniega-Ceballos, A., Sanderson, R. W., Mendo-Pérez, G., Rosado-Fuentes, A., & Chouet, B. A. (2019). "High-broadband seismo-acoustic signature of vulcanian explosions at Popocatépetl volcano, Mexico". *Geophys. Res. Lett.*, 46, 148–157.

McKee, K., Fee, D., Yokoo, A., Matoza, R. S., & Kim, K. (2017). "Analysis of gas jetting and fumarole acoustics at Aso Volcano, Japan". *J. Volcanol. Geotherm. Res.*, 340, 16-29.

McKee, K., Fee, D., Haney, M., Matoza, R. S., & Lyons, J. (2018). "Infrasound signal detection and back azimuth estimation using ground-coupled airwaves on a seismo-acoustic sensor pair". *J. Geophys. Res.*, 123(8), 6826-6844.

Moran, S. C., Matoza, R. S., Garcés, M. A., Hedlin, M. A. H., Bowers, D., Scott, W. E., Sherrod, D. R., and Vallance, J. W. (2008). "Seismic and acoustic recordings of an unusually large rockfall at Mount St. Helens, Washington". *Geophys. Res. Lett.*, 35, L19302.

Mutschlecner, J. P., and Rodney W. Whitaker (2010). "Some atmospheric effects on infrasound signal amplitudes." Infrasound Monitoring for Atmospheric Studies. Springer, Dordrecht. 455-474.

T. B. Neilsen, R. S. Matoza, S. Maher, M. G. McKay, R. Sanderson, G. Valentine, I. Sonder, A. G. Harp, (2019). "Preliminary analyses of seismo-acoustic wave propagation in outdoor field-scale analog volcanic explosions," *J. Acoust. Soc. Am.* 145, 1869.

Ohba, T., Taniguchi, H., Oshima, H., Yoshida, M., & Goto, A. (2002). "Effect of explosion energy and depth on the nature of explosion cloud: a field experimental study". *J. Volcanol. Geotherm. Res.*, 115(1-2), 33-42.

"Qantas cancels flights for a third day". **The Sydney Morning Herald**, 18 April 2010, Archived from the original on 5 June 2011. Sabatier, James M., et al. (**1986**). "Acoustically induced seismic waves." *J. Acoust. Soc. Am.*, 80(2), 646-649.

Spina, L., Morgavi, D., Cannata, A., Campeggi, C., & Perugini, D. (2018). "An experimental device for characterizing degassing processes and related elastic fingerprints: analog volcano seismo-acoustic observations". Rev. Sci. Instrum., 89(5), 055102.

Taddeucci, J., Sesterhenn, J., Scarlato, P., Stampka, K., Del Bello, E., Pena Fernandez, J. J., & Gaudin, D. (2014). "High-speed imaging, acoustic features, and aeroacoustic computations of jet noise from strombolian (and vulcanian) explosions". *Geophys. Res. Lett.*, 41(9), 3096-3102.

Vergniolle, S., & Brandeis, G. (1994). "Origin of the sound generated by strombolian explosions". *Geophys. Res. Lett.*, 21(18), 1959-1962.

Vergniolle, S., Brandeis, G., & Mareschal, J. C. (1996). "Strombolian explosions: 2 eruption dynamics determined from acoustic measurements". *J. Geophys. Res.*, 101(B9), 20449-20466.

Young, S. M., Gee, K. L., Neilsen, T. B., & Leete, K. M. (2015). "Outdoor measurements of spherical acoustic shock decay". *J. Acoust. Soc. Am.*, 138(3), EL305-EL310.